Electronic Supplementary Material (ESI) for Materials Chemistry Frontiers.

Supporting Information

Hydrogen titanate nanosheets-assembled fiber as a new matrix to promote Co-activated PMS process for efficient polychlorinated phenols degradation

Qiaoqiao Ding[#], Mang Niu[#], Hong Su*, Zhanyin Liu, Jianfei Gao, Yanhui Zhao, Chunlei Liu, Yuan Liu*, Chunzhao Liu*

State Key Laboratory of Bio-fibers and Eco-textiles, Institute of Biochemical Engineering, Affiliated Qingdao Central Hospital, College of Materials Science and Engineering, Qingdao University, Qingdao 266071, China.

[*]Corresponding author.

E-mail: su13963924681@163.com (H. Su); liuyuan@qdu.edu.cn (Y. Liu); czliu@qdu.edu.cn (C. Liu)

[#]These authors contributed equally to this paper.

S1 Calculation method

The DFT calculations were carried out using the Vienna Ab-initio Simulation Package (VASP)[S1, 2] with the frozen-core all-electron projector-augment-wave (PAW)[S3, 4] method. The Perdew-Burke-Ernzerhof (PBE)[S5] of generalized gradient approximation (GGA) was adopted to describe the exchange and correlation potential. The cutoff energy for the plane-wave basis set was set to 450 eV. The 2-layer Co_3O_4(311) slab, 3-layer TiO_2(101) slab, mono-layer HTO(101) slab were used. A vacuum region of 20 Å was added above these supercell models to minimize the interactions between neighboring systems. A Co_9O_{12} cluster was placed on HTO(101) slab to built Co_3O_4/HTO composite. The geometry optimizations were performed until the forces on each ion was reduced below 0.01 eV/Å. The Gamma k-point[S6] sampling was used. The van der Waals (vdW) interactions have been considered by using DFT-D3 method of Grimme[S7]. The resulting structures were then used to calculate the electronic structures.

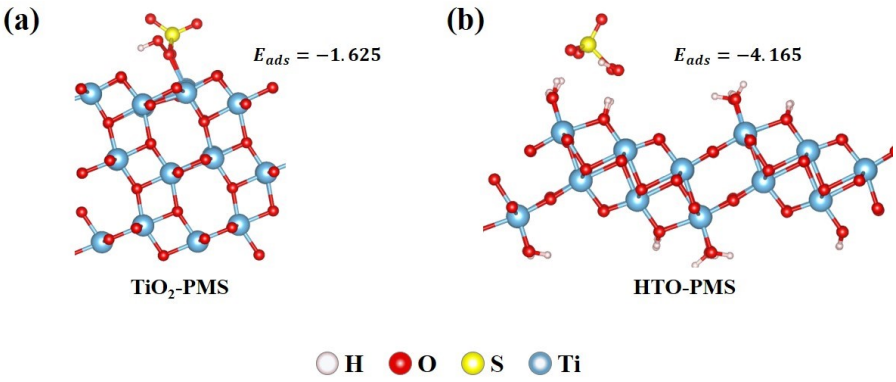

Fig. S1. The DFT optimized structures of PMS adsorption on (a) TiO_2(101) surface and (b) HTO(100) surface.

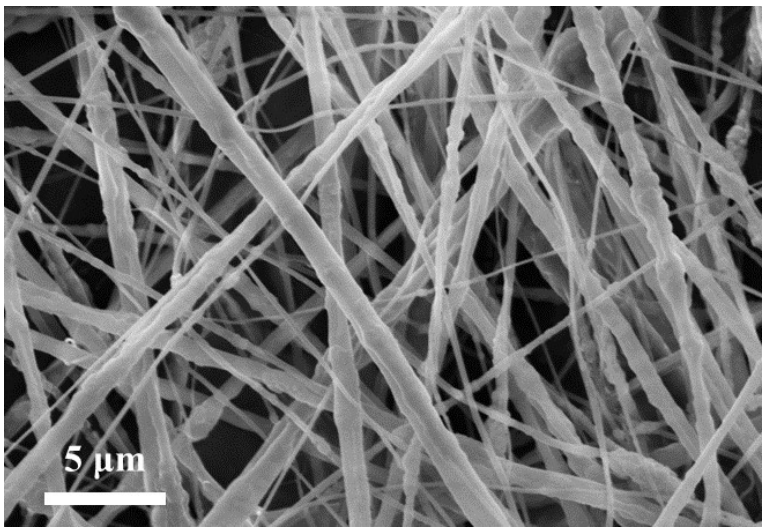

Fig. S2. SEM image of $TiO_2/SiO_2/Co_3O_4$ fibers.

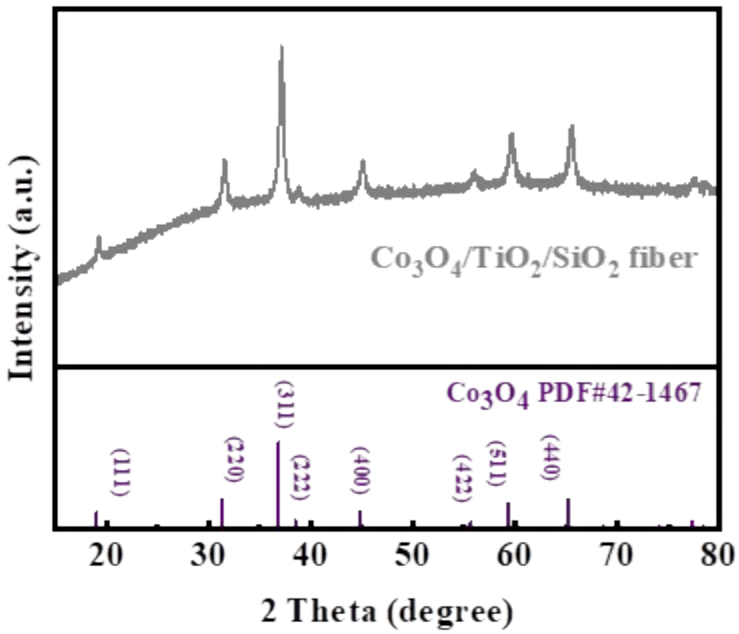

Fig. S3. XRD spectra of $TiO_2/SiO_2/Co_3O_4$ fibers.

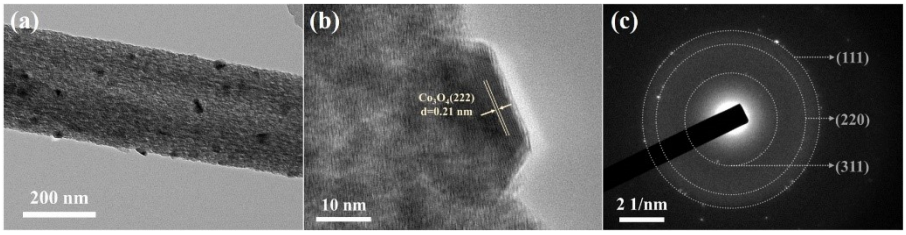

Fig. S4. (a) TEM, (b) HR-TEM, (c) SAED image of $TiO_2/SiO_2/Co_3O_4$ fibers.

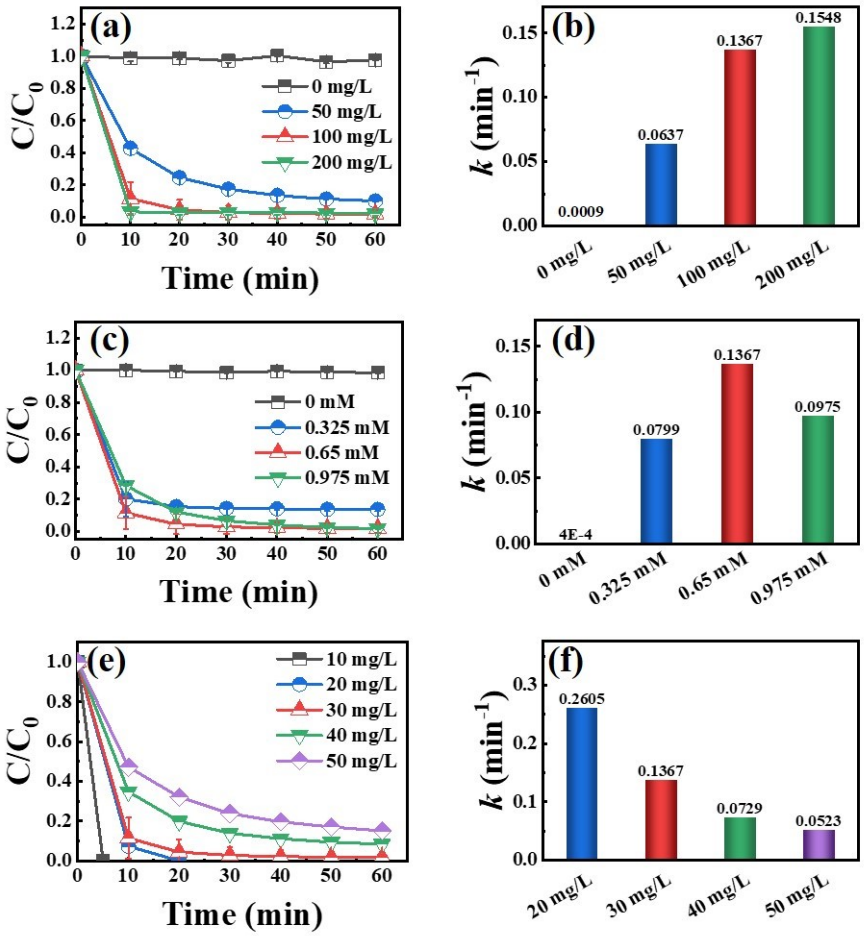

Fig. S5. Effect of the (a, b) Co_3O_4/HTO dosage, (c, d) PMS dosage, (e, f) 2,4-DCP concentration on the removal of 2,4-DCP. Conditions: [2,4-DCP]: 30 mg/L, [catalyst]: 100 mg/L, [PMS]: 0.65 mM, initial pH 5.9, T = 25 °C, unless otherwise specified.

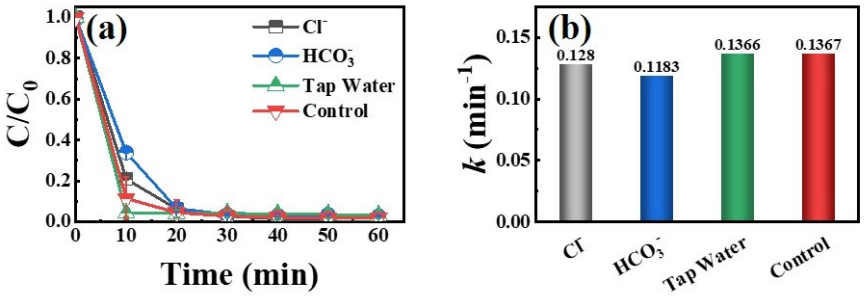

Fig. S6. Effect of coexisting anions on the removal of phenolic. Conditions: [phenolic]: [2,4-DCP]: 30 mg/L, [catalyst]: 100 mg/L, [PMS]: 0.65 mM, initial pH 5.9, T = 25 °C, [ions] = 10 mM.

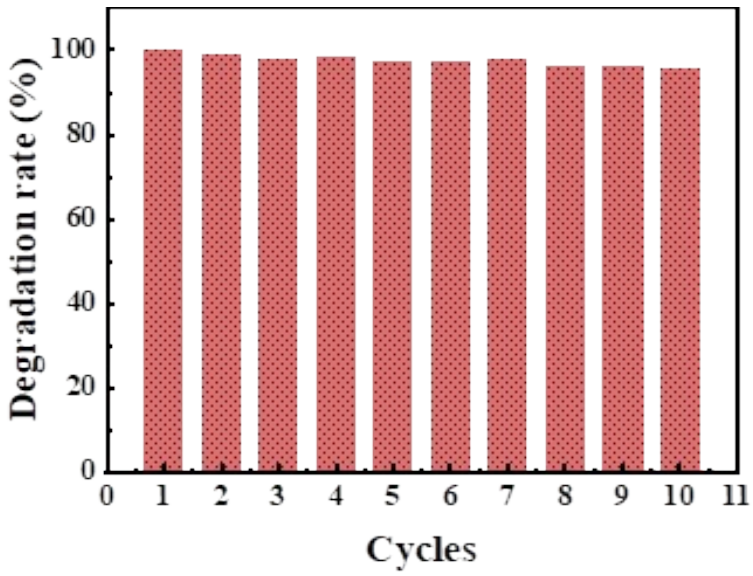

Fig. S7. Effect of the cycle on the removal of phenolic. Conditions: [phenolic]: 10 mg/L, [catalyst]: 100 mg/L, [PMS]: 0.65 mM, initial pH 5.9, T = 25 °C, t = 60 min.

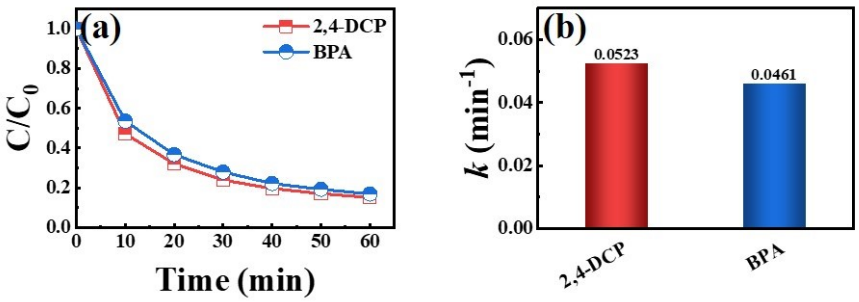

Fig. S8. Effect of the types on the removal of phenolic. Conditions: [phenolic]: 50 mg/L, [catalyst]: 100 mg/L, [PMS]: 0.65 mM, initial pH 5.9, T = 25 °C.

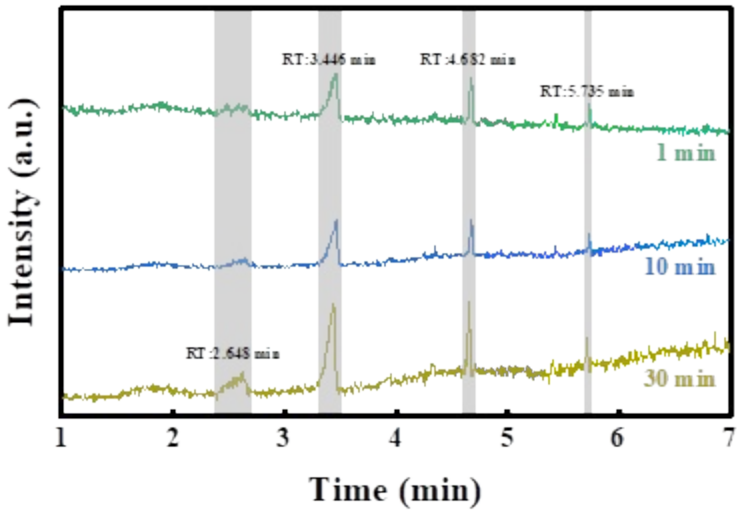

Fig. S9. GC chromatogram of the reaction products during the degradation of 2,4-DCP.

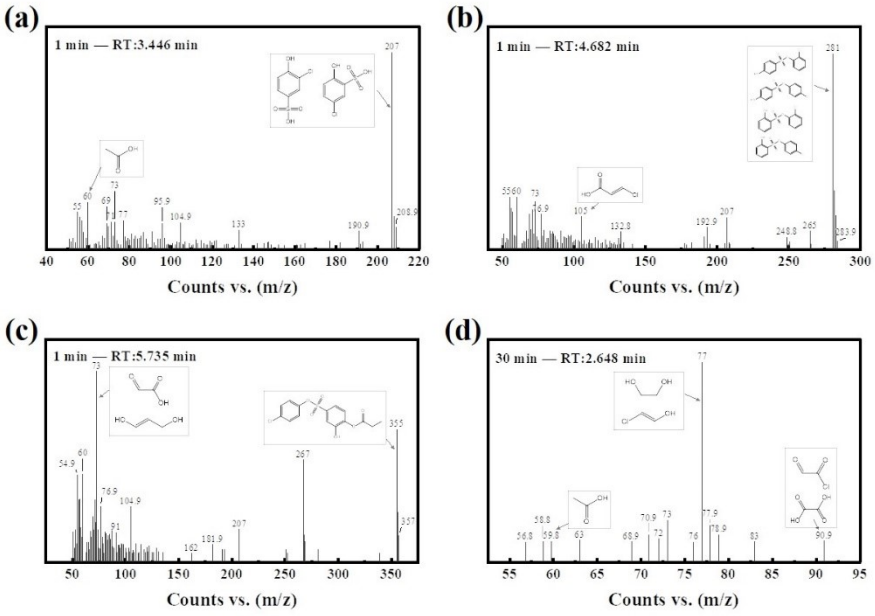

Fig. S10. Mass spectra of the solution samples recorded at 1 min of 2,4-DCP degradation。

Table S1. Degradation intermediate of 2,4-DCP detected by GC-MS.

m/z	Molecular formula	Chemical name	Structural formula
162	$C_6H_4Cl_2O$	2,4-dichlorophenol	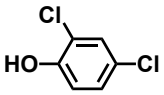
209	$C_6H_5SClO_4$	5-chloro-2-hydroxybenzenesulfonate	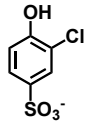
		3-chloro-4-hydroxybenzenesulfonate	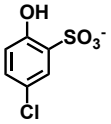
284	$C_{12}H_9SClO_4$	2-chlorophenyl 4-hydroxybenzenesulfonate	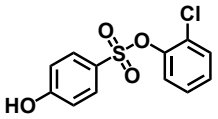
		4-chlorophenyl 4-hydroxybenzenesulfonate	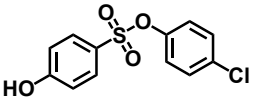
		2-chlorophenyl 2-hydroxybenzenesulfonate	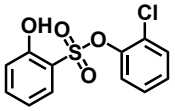
		4-chlorophenyl 2-hydroxybenzenesulfonate	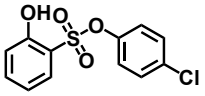
357	$C_{15}H_{13}SClO_6$	4-((4-chlorophenoxy)sulfonyl)-2-hydroxyphenyl propionate	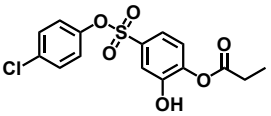
105	$C_3H_3O_2Cl$	(E)-3-chloroacrylic acid	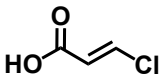
91	C_2HO_2Cl	2-oxoacetyl chloride	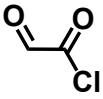
	$C_2H_2O_6$	oxalic acid	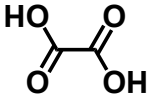
77	C_2H_2OCl	(E)-2-chloroethen-1-ol	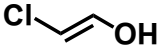
73	$C_2H_2O_3$	2-oxoacetic acid	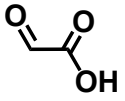
	$C_3H_6O_2$	(E)-prop-1-ene-1,3-diol	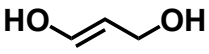

63	$C_2H_6O_2$	ethane-1,2-diol	
60	$C_2H_4O_2$	acetic acid	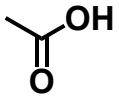
		(Z)-ethene-1,2-diolc	

References

1. G. Kresse and J. Hafner, Ab initio molecular-dynamics simulation of the liquid-metal--amorphous-semiconductor transition in germanium, *Phys. Rev. B*, 1994, **49**, 14251-14269.
2. G. Kresse and J. Furthmüller, Efficient iterative schemes for ab initio total-energy calculations using a plane-wave basis set, *Phys. Rev. B*, 1996, **54**, 11169-11186.
3. P. E. Blöchl, Projector augmented-wave method, *Phys. Rev. B*, 1994, **50**, 17953-17979.
4. G. Kresse and D. Joubert, From ultrasoft pseudopotentials to the projector augmented-wave method, *Phys. Rev. B*, 1999, **59**, 1758-1775.
5. B. Hammer, L. B. Hansen and J. K. Nørskov, Improved adsorption energetics within density-functional theory using revised Perdew-Burke-Ernzerhof functionals, *Phys. Rev. B*, 1999, **59**, 7413-7421.
6. D. J. Chadi, Special points for Brillouin-zone integrations, *Phys. Rev. B*, 1977, **16**, 1746-1747.
7. S. Grimme, Semiempirical GGA-type density functional constructed with a long-range dispersion correction, *J. Comput. Chem.*, 2006, **27**, 1787-1799.